

Probing fully coherent radiation and parton densities using (virtual) photons at the LHC

François Arleo,^{a,*} Djessy Bourgeois,^a Maxime Guilbaud,^a Greg Jackson^a and Víctor Valencia Torres^a

^aSUBATECH UMR 6457 (IMT Atlantique, Université de Nantes, IN2P3/CNRS)

4 rue Alfred Kastler, 44307 Nantes, France

E-mail: francois.arleo@subatech.in2p3.fr, djessy.bourgeois@subatech.in2p3.fr,
maxime.guilbaud@subatech.in2p3.fr, jackson@subatech.in2p3.fr,
victor.valencia@subatech.in2p3.fr

Prompt photon production in pA collisions has long been suggested as a sensitive probe of the nuclear parton distribution functions (nPDFs). In this study, we present recent results on another cold nuclear matter effect, namely fully coherent radiation induced by parton multiple scattering, which may influence the nuclear dependence of prompt photon production. Medium-induced radiation effects, implemented in leading-order direct and fragmentation photon processes, are computed for pPb collisions at the LHC. At backward rapidity, photons are sensitive to fully coherent energy loss (FCEL), while at forward rapidity, fully coherent energy gain (FCEG) plays a crucial role due to the dominance of the $qg \rightarrow q\gamma$ scattering channel. In contrast, for virtual photon production, the impact of fully coherent radiation is marginal, making Drell-Yan (DY) one of the best ways to probe nuclear PDFs. The power of the DY process is demonstrated by reweighting nPDF sets at next-to-leading order using realistic pseudo-data for LHC Run 3.

The European Physical Society Conference on High Energy Physics (EPS-HEP2025)
7-11 July 2025
Marseille, France

*Speaker

1. Introduction

Electroweak probes are excellent tools in high energy proton-nucleus (pA) collisions, with the potential to distinguish genuine modifications of nuclear parton distribution functions (nPDFs) from other cold nuclear matter effects. Among the latter, *fully coherent energy loss* (FCEL) — arising when the emission of a soft gluon has a formation time longer than the nuclear path length — is a robust prediction of QCD [1]. Implications of FCEL have been studied for a variety of hard processes, including quarkonia, light- and heavy-meson production, and even atmospheric neutrinos [2–6].

Because FCEL scales with the energy of the incoming parton, it cannot be neglected and may interfere with clean extractions of nPDFs, especially if those include hadron production data (e.g. charmonium or D -meson [7–9]) in their global fit analyses [10]. This issue is particularly relevant at LHC energies, where energy loss competes with nPDF effects. In contrast, prompt photons are known to undergo minimal final-state interactions making them a cleaner experimental probe of nPDFs [11–13]. However, their leading-order (LO) production mechanism involves a recoiling parton, leaving some room for FCEL (and, as we shall see, *fully coherent energy gain*, FCEG) to affect photon yields in pA collisions.

In these proceedings, we investigate the role of medium-induced coherent energy loss/gain on prompt photon production at the LHC, via the nuclear modification factor,

$$R_{\text{pA}}(y, p_{\perp}) \equiv \frac{1}{A} \frac{d\sigma_{\text{pA}}}{dy dp_{\perp}} \bigg/ \frac{d\sigma_{\text{pp}}}{dy dp_{\perp}}, \quad (1)$$

highlighting the balance of colour charge at forward/backward rapidities (Sec. 2). We also examine the Drell-Yan (DY) process (Sec. 3), which is expected to be far less sensitive to coherent radiation owing to the colourless final state (at leading order) and to the large invariant mass [14]. Using realistic pseudo-data samples, and Bayesian reweighting techniques, we demonstrate the strong constraining power that future LHCb DY measurements could bring to the nPDF programme.

2. Fully coherent radiation effects on prompt photons

In this section we discuss the effects of fully coherent radiation on prompt photon production. The starting point is the calculation of the direct photon production cross section in pp collisions [15],

$$\frac{d\sigma_{\text{pp}}}{dy dp_{\perp}^2} = \sum_{\ell} \frac{d\sigma_{\text{pp}}^{\ell}}{dy dp_{\perp}^2} = \sum_{\ell} \int_{\xi_{\min}}^{\xi_{\max}} d\xi \frac{d\sigma_{\text{pp}}^{\ell}}{dy dp_{\perp}^2 d\xi}, \quad (2)$$

where the sum runs over the various partonic sub-processes $\ell = \{ij \rightarrow \gamma k\}$ at LO in the strong coupling constant, namely Compton scattering and $q\bar{q}$ annihilation, listed in Table 1. We introduce the variable ξ , defined as $\xi = 1/(1 + \exp(y_k - y))$ where y_k is the rapidity of the recoiling parton, which is bounded by $\xi_{\min} \equiv p_{\perp} e^y / \sqrt{s}$ and $\xi_{\max} \equiv 1 - p_{\perp} e^{-y} / \sqrt{s}$. The differential cross section of each sub-process appearing in (2) is given by

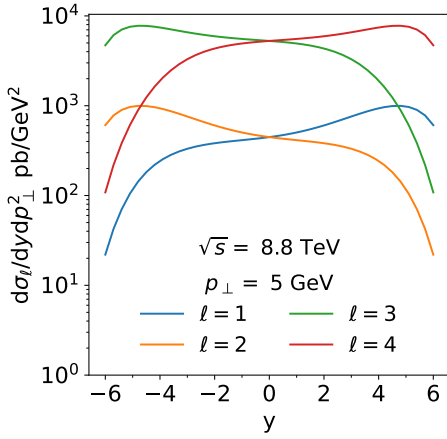
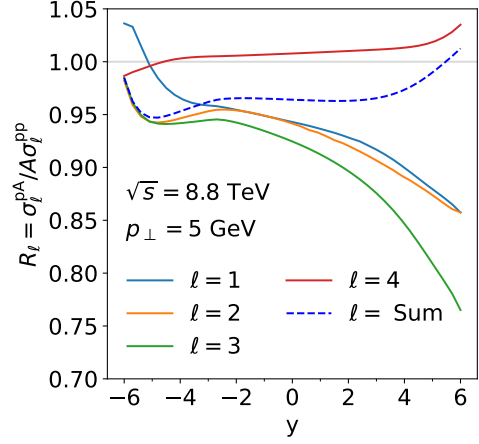
$$\frac{d\sigma_{\text{pp}}^{\ell}}{dy dp_{\perp}^2 d\xi} = \frac{1}{s} \frac{1}{\xi(1-\xi)} f_i^{\text{p}}(x_1, \mu^2) f_j^{\text{p}}(x_2, \mu^2) \frac{d\hat{\sigma}^{\ell}}{d\xi}, \quad (3)$$

where the PDFs f^{p} are evaluated respectively at $x_1 = p_{\perp} e^y / (\xi \sqrt{s})$ and $x_2 = p_{\perp} e^{-y} / ((1-\xi)\sqrt{s})$,

ℓ	Process	R	C_ℓ
1	$q\bar{q} \rightarrow g\gamma$	8	N_c
2	$\bar{q}q \rightarrow g\gamma$	8	N_c
3	$gq \rightarrow q\gamma$	3	N_c
4	$qg \rightarrow q\gamma$	3	$-1/N_c$

Table 1: LO processes for direct γ production.

the factorization scale μ is varied in the range $[p_\perp/2; 2p_\perp]$, and $d\hat{\sigma}^\ell/d\xi$ is the partonic cross section of process ℓ . The cross section in pp collisions at $\sqrt{s} = 8.8$ TeV as a function of y at fixed $p_\perp = 5$ GeV, together with the individual sub-processes, is shown in Figure 1.


Figure 1: Prompt photon differential cross section as a function of y at fixed $p_\perp = 5$ GeV, and for each individual partonic sub-processes.

Figure 2: $R_{\text{pPb}}(y, p_\perp = 5 \text{ GeV})$ for the partonic sub-processes $\ell \in \{1, 2, 3, 4\}$ and when all processes are added (dashed line).

The effects of fully coherent radiation on the differential production cross section in pA collisions can be modeled as¹ [4]

$$\frac{1}{A} \frac{d\sigma_{\text{pA}}(y, p_\perp)}{dy dp_\perp^2} = \sum_\ell \int_{\xi_{\min}}^{\xi_{\max}} d\xi \int_0^{x_{\max}} dx \frac{\mathcal{P}_\ell(x, \xi)}{(1+x)^{s_\ell}} \frac{d\sigma_{\text{pp}}^\ell(y + s_\ell \ln(1+x), p_\perp, \xi)}{dy dp_\perp^2 d\xi}, \quad (4)$$

where $s_\ell \equiv \text{sign}(C_\ell)$ and C_ℓ is a color factor depending on the Casimir of the initial-state partons and that of the irreducible representation R of the final state,² $C_\ell = C_i + C_R - C_j$. The sign of C_ℓ dictates whether the final state experiences fully coherent energy loss (FCEL), $C_\ell > 0$, or fully coherent energy gain (FCEG), $C_\ell < 0$. As can be seen in Table 1, the $\ell = 3$ sub-process, which dominates the cross section at negative rapidity, is sensitive to FCEL (as well as the subdominant $\ell = 1, 2$ channels), while the $\ell = 4$ sub-process, dominant at positive rapidity, is sensitive to FCEG.

¹More generally, the pp cross section in the r.h.s. of (4) can be replaced by a incoherent sum of pp and pn collisions (responsible for isospin effects at backward rapidity [14]), or using genuine nuclear PDF. Here we focus solely on fully coherent radiation, hence the choice of using the pp cross section in (4).

²Since photons are color neutral, there is only one color representation for each sub-process, i.e. $C_R = C_k$.

The quenching weight \mathcal{P}_ℓ appearing in Eq. (4) can be approximated by [16]

$$\mathcal{P}_\ell(x, \xi) \simeq \left| \frac{dI_\ell(x, \xi)}{dx} \right| \exp \left\{ - \int_x^\infty dx' \left| \frac{dI_\ell(x', \xi)}{dx} \right| \right\},$$

where the medium-induced gluon radiation spectrum is taken as [17, 18]

$$x \frac{dI_\ell(x, \xi)}{dx} \simeq C_\ell \frac{\alpha_s}{\pi} \left[\ln \left(1 + \frac{(1 - \xi)^2 Q_s^2}{x^2 p_\perp^2} \right) - \ln \left(1 + \frac{(1 - \xi)^2 Q_{s,p}^2}{x^2 p_\perp^2} \right) \right], \quad (5)$$

with Q_s (resp. $Q_{s,p}$) being the saturation scale in the nucleus (resp. in the proton).³

Using Eq. (4) and Eq. (2) allows for computing the nuclear modification factor R_{pA} , Eq. (1), for each individual sub-process and for the sum. As shown in Figure 2, the shape of R_{pPb} (blue dashed line) results from the interplay of FCEL effects, which tend to suppress the direct photon yield at large negative y (due to sub-processes $\ell \leq 3$, which individual R_{pPb} 's are shown as blue, orange, green lines), while FCEG (due to $\ell = 4$, red line) leads to a slight enhancement, $R_{pPb} \gtrsim 1$, at large positive y .

Figure 3 (left) displays the rapidity dependence of $R_{pPb}(y, p_\perp)$ at fixed $p_\perp = 5$ GeV together with the theoretical uncertainty. It arises mostly from the value of the cold nuclear matter transport coefficient \hat{q} , which sets the magnitude of the saturation scale Q_s . The factorization scale dependence in the PDF, see (3), affects the relative yields of partonic sub-processes⁴ sensitive to FCEL and FCEG and hence contributes to the uncertainty of R_{pPb} , mostly at large positive rapidity. The p_\perp dependence of $R_{pPb}(y, p_\perp)$ at fixed $y = 4$ is shown in Figure 3 (right). As expected, R_{pPb} reaches unity at large p_\perp as the induced gluon spectrum (5) drops rapidly when $p_\perp \gg Q_s$. At low $p_\perp = 3$ GeV, however, the suppression of direct photons lie in the range $0.90 \lesssim R_{pPb} \lesssim 0.95$.

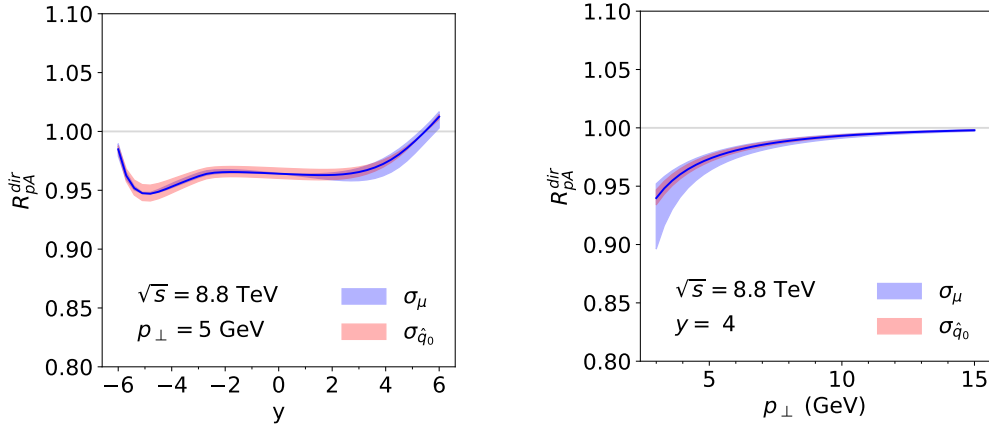


Figure 3: R_{pPb} of direct photon as a function of y at $p_\perp = 5$ GeV (left) and as a function of p_\perp at $y = 4$ (right). The uncertainties reflect the variation of the transport coefficient and that of the factorization scale.

In addition to direct processes, prompt photons can also be produced from the fragmentation of hard partons in QCD processes, $ij \rightarrow kl(\rightarrow \gamma)$. Because of the parametric dependence of

³The expressions used for Q_s and x_{\max} can be found e.g. in Ref. [4].

⁴The distinction between various partonic sub-processes is scale-dependent and ambiguous beyond the leading order.

the fragmentation function, $D_l^\gamma = \mathcal{O}(\alpha/\alpha_s)$, fragmentation photons contribute in principle to the same order as direct photons in perturbation theory. Their contribution, however, is strongly suppressed due to isolation requirements, used in the experiments to suppress the background from neutral meson decays (in what follows the amount of hadronic energy deposited within the cone of radius $R = 0.4$ centered around the photon is required to be less than 10% of the photon p_\perp). The FCEL/G effects on fragmentation photons have been computed systematically along the lines of Ref. [4] on light hadron production. The relative yields of all partonic sub-processes and the shape of their rapidity distributions were evaluated using the JETPHOX Monte-Carlo generator [15]. The resulting R_{pPb} , together with those from direct photons and the sum of both components is shown in Figure 4. Although the theoretical uncertainty on R_{pPb} is slightly enlarged, the inclusion of fragmentation photons does not dramatically affect its magnitude.

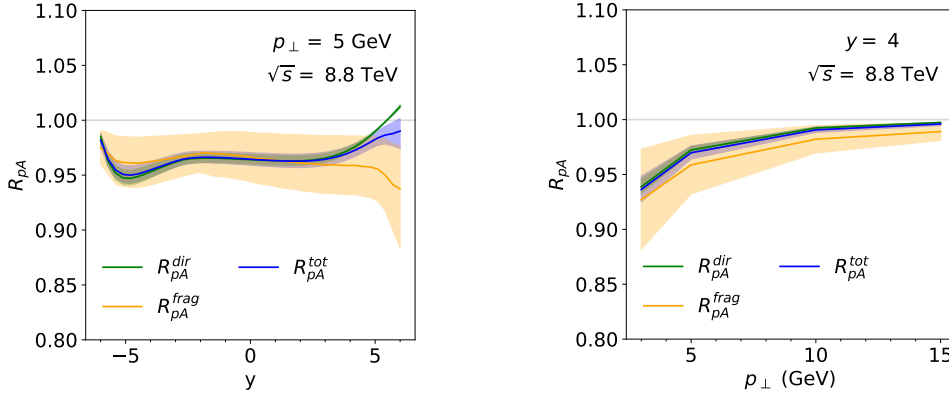


Figure 4: R_{pPb} of direct (green band), fragmentation (yellow band) and total prompt photons (blue band) as a function of y at $p_\perp = 5$ GeV (left) and as a function of p_\perp at $y = 4$ (right).

3. nPDF constraints from virtual photons

Closely related to prompt photons is the Drell-Yan (DY) process whereby the invariant mass (M) of the photon is non-zero. At leading order, $q\bar{q} \rightarrow \gamma^*$, DY is insensitive to FCEL due to the absence of a recoiling parton [14]. Real emissions start at NLO, leading to $\Delta E_{\text{FCEL}} \propto Q_s/\sqrt{M^2 + p_\perp^2} \ll 1$, and consequently the role of nPDFs prevails. Low-mass DY in pA collisions at the LHC would thus be an ideal probe of nuclear shadowing at small- x , being largely uncontaminated by energy loss effects like FCEL. We demonstrate this explicitly by generating pseudo-data for $R_{\text{pPb}}(y)$ at the collisional energy of $\sqrt{s_{\text{NN}}} = 8.8$ TeV, and apply reweighting techniques to existing nPDF sets. (A similar demonstration was made for future EIC measurements in Ref. [19].)

First let us describe our recipe for producing the pseudo-data, using a setup in accordance with Runs 3 and 4 at LHCb [20]. Here we focus on the range $5 < M < 9$ GeV, and p_\perp -integrated result (to avoid complications such as the Cronin effect). To simplify notation, we refer to the cross-section as rapidity differential, i.e. $\sigma_i \equiv d\sigma_i/dy$ where i denotes the nPDF member set and j will be reserved

for the relevant rapidity bin y_j , $\sigma_i(j) = d\sigma_i(y_j)/dy$. We consider the following rapidity bins,⁵

$$\begin{aligned} \text{backward:} & \quad [-5, -4.5], [-4.5, -4], [-4, -3.5], [-3.5, -3]; \\ \text{forward:} & \quad [+2, +2.5], [+2.5, +3], [+3, +3.5], [+3.5, +4]. \end{aligned} \quad (6)$$

A perturbative prediction for $\sigma_i^{\text{pp}}(j)$ and $\sigma_i^{\text{pPb}}(j)$ can be obtained with the DYTurbo code [21] (adapted for asymmetric collisions). We do so at NLO, with factorization and renormalization scales $\mu^2 = \mathcal{O}(M^2)$, and focus on the sets provided⁶ by nNNPDF3.0 [8]. We denote the corresponding R_{pA} from Eq. (1) by $R(j)$, for which the statistical error δR can be estimated from

$$\frac{\delta R(j)}{R(j)} = \sqrt{\left[\frac{1}{N_{i=0}^{\text{pPb}}(j)} + \frac{1}{N_{i=0}^{\text{pp}}(j)} \right] \left[1 + \frac{1}{(S/B)_{j,\text{eff}}} \right]}, \quad (7)$$

where we use the signal-to-background ratio $(S/B)_{j,\text{eff}} \simeq 1/30$, as compatible with Ref. [20]. From the cross-sections (output by DYTurbo), one may then estimate

$$N_i^{\text{pp}}(j) = \mathcal{A}\epsilon \times \mathcal{L}_{\text{pp}} \times \sigma_i^{\text{pp}}(j); \quad N_i^{\text{pPb}}(j) = \mathcal{A}\epsilon \times \mathcal{L}_{\text{pPb}} \times \sigma_i^{\text{pPb}}(j), \quad (8)$$

where acceptance times efficiency $\mathcal{A}\epsilon \approx 0.9$ and foreseen luminosities of $\mathcal{L}_{\text{pp}} = 104 \text{ pb}^{-1}$ and $\mathcal{L}_{\text{pPb}} \approx 250 \text{ nb}^{-1}$. With these values, we obtain a relative uncertainty of $\sim 5\%$ in Eq. (7). Finally, we sampled data from a normal distribution (\mathcal{N}) centered on \hat{R} and with statistical variance δR^2 :

$$R_{\text{data}}(j) \sim \mathcal{N}(\hat{R}(j), \delta R^2(j)), \quad (9)$$

where the mean value is given by the central nPDF set $\hat{R}(j) \equiv R_{\text{pA}}^{\text{nNNPDF}}(j)|_{i=0}$.

Next, we apply the reweighting method using the Bayesian approach (as applicable to NNPDF sets) which is briefly summarised here. (A more thorough discussion of both Bayesian and Hessian methods can be found, e.g. in Ref. [22].) Given a large ensemble of (n)PDFs f_i , $i = 1 \dots N_{\text{rep}}$, sampled with equal weights from the underlying functional probability distribution, the expectation value and variance of an observable may be computed from

$$\langle \mathbb{O} \rangle_{\text{old}} = \frac{1}{N_{\text{rep}}} \sum_{i=0}^{N_{\text{rep}}} \mathbb{O}[f_i], \quad \delta \langle \mathbb{O} \rangle_{\text{old}} = \sqrt{\frac{1}{N_{\text{rep}}} \sum_{i=0}^{N_{\text{rep}}} (\mathbb{O}[f_i] - \langle \mathbb{O} \rangle_{\text{old}})^2}. \quad (10)$$

Given new measurements, the χ_i^2 for each replica can be calculated, which gives a notion of “how far” that replica is from reproducing the data. If the data are uncorrelated,

$$\chi_i^2 = \sum_{j=1}^{N_{\text{data}}} \left[\frac{R_{\text{data}}(j) - R_{\text{th}}^i(j)}{\delta R_{\text{data}}(j)} \right]^2, \quad (11)$$

for which each i is assigned the weight

$$w_i = \frac{1}{\mathcal{D}} (\chi_i^2)^{(N_{\text{data}}-1)/2} e^{-\chi_i^2/2}; \quad \mathcal{D} \equiv \sum_{i=1}^{N_{\text{data}}} (\chi_i^2)^{(N_{\text{data}}-1)/2} e^{-\chi_i^2/2}, \quad (12)$$

where the normalisation constant \mathcal{D} ensures that $\sum_i w_i = 1$. This gives us “reweighted” predictions for a given quantity, namely

$$\langle \mathbb{O} \rangle_{\text{new}} = \sum_{i=0}^{N_{\text{rep}}} w_i \mathbb{O}[f_i], \quad \delta \langle \mathbb{O} \rangle_{\text{new}} = \sqrt{\sum_{i=0}^{N_{\text{rep}}} w_i (\mathbb{O}[f_i] - \langle \mathbb{O} \rangle_{\text{new}})^2}. \quad (13)$$

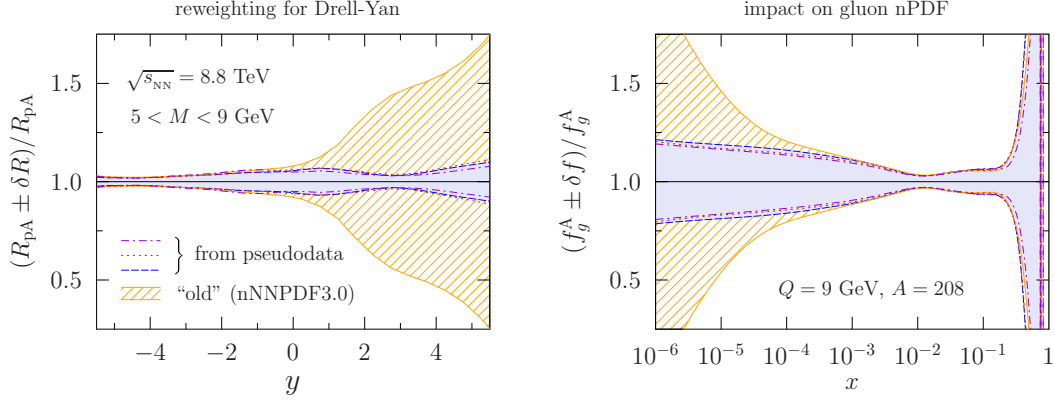


Figure 5: Left: relative error in the predicted R_{pA}^{DY} as a function of rapidity, before and after reweighting. Right: the same, but for the gluon nPDF $f_g^A(x, Q = 9 \text{ GeV})$ as a function of x . Note that in both panels, only the uncertainty in the nPDFs is shown and calculated according to Eq. (10) and Eq. (13).

The observable corresponding to the pseudo-data, $\odot = R_{p\text{Pb}}^{\text{DY}}$, is displayed in Figure 5. We generate three independent sets of pseudo-data, which each lead to slightly varying predictions for the modification factor. However, the relative improvement in the error⁷ is similar in all cases with and especially significant at forward rapidity (by construction). The consequence of these reweightings for the gluon nPDF is also shown, demonstrating the constraining power at small x (and similarly for the quarks, not shown). Although slightly less stringent than results obtained with D -mesons, it may be more reliable as DY is comparatively unaffected by FCEL.

4. Conclusion

In summary, we have estimated influence of fully coherent energy loss and energy gain on prompt photon production in pA collisions. Although these effects are generally small, they are not negligible (especially at low p_\perp and backward rapidity $y < 0$), and arise from a subtle interplay between energy loss and energy gain mechanisms. On the other hand, the DY process remains largely impervious to medium induced coherent gluon radiation, making it one of the most promising probes of nuclear PDFs. Using realistic run 3 pseudo-data, we performed an NLO reweighting study and found that DY measurements can provide significant constraints on both quark and gluon densities at small- x .

Acknowledgments

We thank Jean-Philippe Guillet for discussions and Michael Winn for discussions and for providing us with the acceptance/efficiency and luminosity expected with LHCb at Run 3. G.J. is supported by the Agence Nationale de la Recherche (ANR) under grant ANR-22-CE31-0018.

⁵Strictly speaking, the cross-section for bin y_j ($j = 1, \dots, 8$) is given by $\frac{1}{\Delta y} \int_{y_{\min}}^{y_{\max}} dy \frac{d\sigma(y)}{dy}$.

⁶Specifically, we use those sets which do not use LHCb D -meson data and having $N_{\text{rep}} = 250$ replicas.

⁷We recognize that Ref. [8] advocates computing the error with confidence level intervals rather than the variance (see Sec. 7.2 of that work). However, we use Eq. (13) for simplicity and because our purpose here is not to make actual predictions but to motivate future measurements.

References

- [1] F. Arleo, S. Peigné and T. Sami, *Revisiting scaling properties of medium-induced gluon radiation*, *Phys. Rev.* **D83** (2011) 114036 [[1006.0818](#)].
- [2] F. Arleo and S. Peigné, *J/ψ suppression in pA collisions from parton energy loss in cold QCD matter*, *Phys. Rev. Lett.* **109** (2012) 122301 [[1204.4609](#)].
- [3] F. Arleo and S. Peigné, *Quenching of light hadron spectra in pA collisions from fully coherent energy loss*, *Phys. Rev. Lett.* **125** (2020) 032301 [[2003.01987](#)].
- [4] F. Arleo, F. Cougoulic and S. Peigné, *Fully coherent energy loss effects on light hadron production in pA collisions*, *JHEP* **09** (2020) 190 [[2003.06337](#)].
- [5] F. Arleo, G. Jackson and S. Peigné, *Impact of fully coherent energy loss on heavy meson production in pA collisions*, *JHEP* **01** (2022) 164 [[2107.05871](#)].
- [6] F. Arleo, G. Jackson and S. Peigné, *Depletion of atmospheric neutrino fluxes from parton energy loss*, *Phys. Lett. B* **835** (2022) 137541 [[2112.10791](#)].
- [7] K.J. Eskola, P. Paakkinen, H. Paukkunen and C.A. Salgado, *EPPS21: A global QCD analysis of nuclear PDFs*, *The European Physical Journal C* **82** (2022) 413 [[2112.12462](#)].
- [8] R. Abdul Khalek, R. Gauld, T. Giani, E.R. Nocera, T.R. Rabemananjara and J. Rojo, *nNNPDF3.0: evidence for a modified partonic structure in heavy nuclei*, *Eur. Phys. J. C* **82** (2022) 507 [[2201.12363](#)].
- [9] P. Duwentäster, T. Ježo, M. Klasen, K. Kovařík, A. Kusina, K.F. Muzakka et al., *Impact of heavy quark and quarkonium data on nuclear gluon PDFs*, *Phys. Rev. D* **105** (2022) 114043.
- [10] F. Arleo et al., *Nuclear Cold QCD: Review and Future Strategy*, [2506.17454](#).
- [11] F. Arleo and T. Gousset, *Measuring gluon shadowing with prompt photons at RHIC and LHC*, *Phys. Lett. B* **660** (2008) 181 [[0707.2944](#)].
- [12] F. Arleo, K.J. Eskola, H. Paukkunen and C.A. Salgado, *Inclusive prompt photon production in nuclear collisions at RHIC and LHC*, *JHEP* **04** (2011) 055 [[1103.1471](#)].
- [13] I. Helenius, K.J. Eskola and H. Paukkunen, *Probing the small-x nuclear gluon distributions with isolated photons at forward rapidities in pPb collisions at the LHC*, [1406.1689](#).
- [14] F. Arleo and S. Peigné, *Disentangling Shadowing from Coherent Energy Loss using the Drell-Yan Process*, *Phys. Rev.* **D95** (2017) 011502 [[1512.01794](#)].
- [15] P. Aurenche, M. Fontannaz, J.-P. Guillet, É. Pilon and M. Werlen, *A new critical study of photon production in hadronic collisions*, *Phys. Rev.* **D73** (2006) 094007 [[hep-ph/0602133](#)].
- [16] F. Arleo and S. Peigné, *Heavy-quarkonium suppression in pA collisions from parton energy loss in cold QCD matter*, *JHEP* **03** (2013) 122 [[1212.0434](#)].

- [17] G. Jackson, S. Peigné and K. Watanabe, *Coherent gluon radiation: beyond leading-log accuracy*, *JHEP* **05** (2024) 207 [2312.11650].
- [18] F. Arleo, D. Bourgeais and G. Jackson, in preparation.
- [19] N. Armesto, T. Cridge, F. Giuli, L. Harland-Lang, P. Newman, B. Schmookler et al., *Impact of inclusive electron ion collider data on collinear parton distributions*, *Phys. Rev. D* **109** (2024) 054019 [2309.11269].
- [20] M. Winn, “LHCb projections for proton-lead collisions during LHC Runs 3 and 4.” <http://cds.cern.ch/record/2648625>.
- [21] S. Camarda et al., *DYTurbo: Fast predictions for Drell-Yan processes*, *Eur. Phys. J. C* **80** (2020) 251 [1910.07049].
- [22] H. Paukkunen and P. Zurita, *PDF reweighting in the Hessian matrix approach*, *JHEP* **12** (2014) 100 [1402.6623].